Multiple strong field ionization of metallocenes: Applicability of ADK rates to the production of multiply charged transition metal (Cr, Fe, Ni, Ru, Os) cations

Multiple strong field ionization of metallocenes: Applicability of ADK rates to the production of multiply charged transition metal (Cr, Fe, Ni, Ru, Os) cations

Eri Murakami, Ryuji Mizoguchi, Yusuke Yoshida, Akihiro Kitashoji, Nobuaki Nakashima, Tomoyuki Yatsuhashi

Citation	Journal of Photochemistry and Photobiology A: Chemistry, 369; 16-24
Issue Date	2019-01-15
Type	Journal Article
Textversion	author
Highlights	·Multiply charged transition metal cations up to 8+ are produced from metallocenes. ·Singly charged metal cations liberated from the excited metallocene are further ionized by tunneling. ·Cations were produced from metallocene at laser intensity lower than that expected by ADK theory for bare metal atoms.
Rights	© 2018 Elsevier B.V. This manuscript version is made available under the CC-BY-NC-ND 4.0 License. https://creativecommons.org/licenses/by-nc-nd/4.0/ . This is the accepted manuscript version. The following manuscript has been accepted by Journal of Photochemistry and Photobiology A: Chemistry. The article has been published in final form at https://doi.org/10.1016/j.jphotochem.2018.10.009
DOI	10.1016/j.jphotochem.2018.10.009

Self-Archiving by Author(s)
Placed on: Osaka City University

Multiple strong field ionization of metallocenes: Applicability of ADK rates to the production of multiply charged transition metal (Cr, Fe, Ni, Ru, Os) cations

Eri Murakami,[†] Ryuji Mizoguchi,[‡] Yusuke Yoshida,[†] Akihiro Kitashoji,[†] Nobuaki Nakashima,[†] and Tomoyuki Yatsuhashi[*,†]

Department of Chemistry, Graduate School of Science, Osaka City University, 3-3-138 Sugimoto, Sumiyoshi, Osaka 558-8585 Japan, Sakurazuka High School, 4-1-1 Nakasakurazuka, Toyonaka, Osaka 561-0881 Japan

*To whom correspondence should be addressed. Telephone: +81-6-6605-2554. FAX: +81-6-6605-2522. E-mail: tomo@sci.osaka-cu.ac.jp (T.Y.)

[†]Graduate School of Science, Osaka City University.

[‡]Sakurazuka High School

Abstract

The reactions of a neutral molecule with a singly charged ion in the gas phase have been studied extensively in connection with catalytic reactions, interstellar and planetary atmospheric chemistry, and the MALDI process. In contrast, the reactions of a neutral molecule with a multiply charged ion have rarely been reported, in part because it is difficult to produce such ions in abundance. In this study, we report the production of multiply charged transition metal cations from metallocenes in intense femtosecond laser fields. The most highly charged metals observed at 3×10^{15} W cm^{-2} are Cr^{6+}, Fe^{6+}, Ni^{6+}, Ru^{7+}, and Os^{8+}. The production of carbon-containing cations originating in cyclopentadienyl ligands is small relative to that of metal cations because the ligands are dominantly liberated as neutral fragments. Metal cations having higher charges are formed by the sequential (stepwise) tunnel ionization of the singly (doubly) charged metal cations that are liberated from the excited metallocene cation (dication). The experimentally measured and theoretically calculated saturation intensities of cation generation are compared. The quasiclassical tunneling theory under a single active electron approximation has been known to underestimate the saturation intensity of singly charged metal cations. However, we investigate that this theory overestimates the saturation intensity of multiply charged metal cations referred to as an enhanced

ionization. Moreover, the degree of overestimation becomes significant as the charge number of the metal cation increases. The characteristic deviation of the theoretical predictions from the experimental results is a key issue for the future clarification of the multiple-tunneling ionization processes. We suggest that the polarizabilities depending on the charge number, and presumably the excitation of cations, might be important in the multiple ionization of transition metals. In addition, the production of multiply charged metal cations in abundance, and the reduced production of carbon and hydrocarbon fragment cations achieved by femtosecond laser ionization, will be valuable as sources of multiply charged metal cations for further ion–molecule reaction studies.

1. Introduction

Ion–molecule reactions [1, 2] have been of great interest in connection with catalytic reactions [3, 4], interstellar and planetary atmospheric chemistry [5-8], the MALDI process [9], and so on. The reactions between a neutral molecule and a singly charged cation such as a transition metal cation have been the focus of these studies. A guided ion beam tandem mass spectrometer [10, 11] and Fourier transform ion cyclotron resonance have been utilized to investigate ion–molecule reactions [12, 13]. In contrast, the reactions between a neutral molecule and a doubly [14] or triply [15] charged atomic cation, or a molecular dication [16-19], have rarely been reported. This is partly because the charge transfer reaction dominates the bond-forming reaction due to the high potential energy and high electron affinity of multiply charged cations. Although such exothermic and exotic reactions are attractive subjects [16, 20-23], there remain a number of difficulties that need to be overcome.

First, the efficient production of multiply charged species is necessary. The production of multiply charged molecular cations has been accomplished by using several methods, such as electron ionization [24, 25], vacuum ultraviolet light irradiation [26], collision with high-energy projectiles [27, 28], ion beam sputtering of a solid surface [29, 30], and femtosecond laser ionization [31-37]. The highest charge number of an intact

4

molecule obtained to date is 12 (C_{60}^{12+}) by femtosecond laser ionization (1800 nm, 70 fs,

10^{15} W cm^{-2}) [38]. However, the confinement of multiple positive charges in a small

molecule is difficult due to strong Coulomb repulsions. Therefore, most multiply charged

molecular cations are metastable in nature and easily dissociate into fragments [39, 40].

In other words, we can produce multiply charged atomic cations such as C^{4+} and Si^{4+} via

Coulomb explosion of multiply charged molecular cations, but hydrocarbon fragment

cations are usually formed in abundance [41].

There is another difficulty in the cases of metal cation productions by the above-

mentioned techniques: the reactants should be introduced in a reaction chamber as a vapor

sample. In contrast to volatile organic compounds, the vaporization of pure metals

requires high temperature. For example, the boiling point of osmium is 5285 K. We need

to raise the temperature to at least 2520 K to achieve vapor pressure above 10^{-5} Pa. Even

when vapor pressure is sufficient, the deposition of metals on the experimental apparatus

becomes a serious problem. The laser ablation of metals is a possible means to avoid these

difficulties [42]. The use of organometallic compounds in what is known as the MIVOC

(metal ions from volatile compounds) method is another alternative means [43].

Organometallic complexes such as metallocene (MCp_2, M = metal, Cp = η^5-C_5H_5) and/or

carbonyl complexes having relatively high vapor pressure at room temperature are

promising candidates. Another choice is metal alkyl complexes, although some of these molecules can be difficult to handle.

In order to form singly charged metal cations from metallocenes, multiphoton ionization by using UV nanosecond laser pulses is a very advantageous approach [44-48]. By tuning the wavelength of a laser pulse, only a metal cation is selectively produced. This is attributable to the fact that a neutral metal atom is liberated from the excited state of metallocene followed by resonant ionization. Unfortunately, multiply charged metal cations are not formed due to the insufficient energy deposition by nanosecond laser pulses. For the production of multiply charged atomic cations, electron beam ion trap and electron cyclotron resonance have been utilized [49-51]. However, these powerful ionization methods form not only multiply charged metal cations but also carbon and hydrocarbon cations originating in organic ligands [52]. The contamination as well as adsorption of such carbon-based materials on the reaction chamber are not favorable. Abundant production of multiply charged metal cations, combined with negligible amounts of carbon and fragment cations, are desirable as the ion source for further ion–molecule reaction studies. In our previous communication, we demonstrated the generation of multiply charged iron cations with small amounts of carbon and hydrocarbon cations from ferrocene in intense laser fields [53]. Moreover, the production

of multiply charged iron cations requires less laser intensity than theoretically expected for iron atoms. In the present study, we report the production of multiply charged cations of other transition metals such as chromium, nickel, ruthenium, and osmium. The experimentally measured and theoretically calculated saturation intensities of the multiply charged transition metal cations produced are compared and discussed.

2. Materials and methods

Chromocene ($CrCp_2$, Aldrich, 95%), ferrocene ($FeCp_2$, Aldrich, 98%), nickelocene ($NiCp_2$, Tokyo Chemical Industry, 98%), and xenon (Japan Air Gases, 99.99%) were each introduced to an ionization chamber by a leak valve at 296 K. Ruthenocene ($RuCp_2$, Aldrich, 98%) was kept at 348 K in order to maintain sufficient vapor pressure. Osmocene ($OsCp_2$, Wako) kept at 296 K was directly introduced into a vacuum chamber by using an organic deposition cell (KOD-Cell, Kitano Seiki). The chamber pressure was monitored 20 cm away from the laser focus point with a cold cathode pressure gauge. The base pressure of the ionization chamber and the time-of-flight chamber was below 5×10^{-7} Pa. The pressure of metallocenes in the ionization chamber was kept below 5.5×10^{-5} Pa during the experiments to avoid the space-charge effect. The pressure of the time-of-flight mass chamber was 10 times below the ionization

chamber by differential pumping to avoid collision-induced fragmentation.

The experimental details have been described elsewhere [37]. Briefly, the multiple ionization of metallocene and xenon was carried out with a 45-fs pulse centered at 0.8 μm (Thales laser, Alpha 100/1000/XS hybrid), and the ions were detected by a liner mode of Wiley-Mclaren time-of-flight mass spectrometer (TOF-MS, Toyama, KNTOF-1800). The acceleration voltage was 4000 V, and the extraction field potential 833 V cm^{-1} was optimized to have the highest mass resolution and highest signal intensity. The resolution ($m/\Delta m$, fwhm) was 1620 at $m/z = 129$. A slit of 500 μm width was located on the extraction plate perpendicular to the laser propagation direction in order to collect the ion that was generated in the most tightly focused point of the laser beam (achieving ion collection from axially symmetric parallel beam geometry). The ion yield was obtained by integrating over the appropriate peaks in the time-of-flight spectrum. The direction of the laser polarization (linear) and the TOF axis was parallel. The laser beam was focused into the ionization chamber with a planoconvex quartz lens of 200 mm focusing length. The actual laser intensity of the linear polarized pulse at the focus was determined by measuring the saturation intensity, I_{sat} of xenon (1.1×10^{14} W cm^{-2} for a 45 fs pulse) by the method of Hankin et al. [54], and the error in the determination of absolute laser intensity was about ±10%. The ions of the metallocenes were measured successively after

the measurement of I_{sat} of xenon without, between two runs, changing experimental conditions.

3. Results and Discussion

3.1. Ionization of metallocenes in femtosecond laser fields

Fig. 1 shows the time-of-flight mass spectra of MCp_2 (M = Cr, Ni, Ru, Os) measured above 10^{15} W cm^{-2}. The mass spectrum of $FeCp_2$ was reported in our previous report [53]. The dominant species in the mass spectra were singly and doubly charged molecular cations (MCp_2^+, MCp_2^{2+}), metal cations, H^+, H_2^+, and carbon ions (C^{3+}, C^{2+}, C^+). MCp^+ was identified but the amounts of Cp^+ ($m/z = 65$), $C_3H_n^+$, $C_2H_n^+$, and CH^+ were negligible. As the amounts of carbon-containing fragments were very small relative to the amounts of metal cations, it is reasonable to conclude that most cyclopentadienyl ligands are detached as neutral fragments. The multiply charged metal cations were definitively identified by the mass-to-charge ratio (m/z), isotope pattern, and narrower peak width than those of lower-charged cations. The mass spectra of the most highly charged metals (Cr^{6+}, Ni^{6+}, Ru^{7+}, and Os^{8+}) are shown in Fig. S1. The most highly charged iron was Fe^{6+}, whose mass spectrum was reported elsewhere [53]. Although some of their peaks overlapped with the lower-charged cations and the signal-to-noise ratios were small, the

9

experimentally observed isotopic structure coincided well with the natural abundance of the isotopes of the corresponding atoms. The xenon with the highest charge observed in this study was Xe^{7+}.

It should be mentioned that metal cations having higher charges are formed if we use metal clusters as reactants. The ionization of metal clusters in high intensity femtosecond laser field have been extensively studied by Castleman and coworkers. They have investigated the maximum observed charge state (MOCS) for various metals. For example, MOCS of Ti, V, Cr, Nb, and Ta obtained either from metal oxide [55] or from metal carbide clusters [56] at $\sim 1 \times 10^{15}$ Wcm^{-2} (624 nm, 100 fs) were 10, 9, 8, 11, and 11, respectively. The same MOCS was obtained from pure metal (Nb, Ta) clusters [57]. The appearance of those charge states is dependent on the stability of clusters [58], and is the results of intracluster interactions referred to as an "enhanced ionization".

Here we consider the interactions between intense femtosecond laser fields and isolated metallocenes as well as the origins of metal cations. The lowest electronically excited levels of metallocene are accessible by two- or three-photon processes with 0.8-μm photons. As the laser intensity increases, MCp_2^+ and MCp_2^{2+} form. The first and second leaving electrons belong to metal d-derived molecular orbitals of MCp_2: $CrCp_2$, $(a_{1g})^1(e_{2g})^3$; $FeCp_2$, $RuCp_2$, $OsCp_2$, $(a_{1g})^2(e_{2g})^4$; $NiCp_2$, $(a_{1g})^2(e_{2g})^4(e_{1g})^2$. As MCp_2^{3+} is not

detected by time-of-flight mass spectroscopy, its lifetime is shorter than the acceleration

time of our mass spectrometer (<1 μs). Recently, the dissociation dynamics of $FeCp_2$

exposed to intense femtosecond laser fields (780 nm, $2\times10^{13}-1.4\times10^{14}$ W cm^{-2}) have

been demonstrated by time-resolved XUV absorption spectroscopy [59]. Element-

specific absorption spectroscopy (Fe 3p) has revealed the formation of Fe^+ from the

excited $FeCp_2^+$ within 240 fs ($\geq6\times10^{13}$ W cm^{-2}). This result is quite informative with

respect to the origin of multiply charged metal cations. Since only small amounts of

carbon cations are formed, the formation of multiply charged molecular cations is not

expected. The generation of multiply charged metal cations directly from multiply

charged molecular cations by Coulomb explosion is unlikely. Therefore, the origin of

multiply charged iron cations may be the further ionization of Fe^+. However, the Fe^+

formed from the excited $FeCp_2^+$ was presumably not further excited and/or was not

ionized efficiently within the 45-fs laser pulses used in our study. Therefore, the possible

sources that generate Fe^+ within 45-fs are the more highly excited states of $FeCp_2^+$.

Another possible source of fast-evolving Fe^+ is the excited $FeCp_2^{2+}$ as we suggested in

our previous work [53].

We have reported that the yields of $FeCp_2^+$ are saturated at 6×10^{13} W cm^{-2}. The

relative abundances of $FeCp_2^+$, $FeCp_2^{2+}$, and Fe^+ at 6×10^{13} W cm^{-2} are 100, 10, and 8.5,

respectively [53]. Those of $FeCp_2^+$, $FeCp_2^{2+}$, Fe^+, and Fe^{2+} at 1×10^{14} W cm^{-2}, where the

yields of $FeCp_2^{2+}$ are saturated, are 100, 25, 23, and 5, respectively [53]. In the case of

the time-resolved XUV absorption spectroscopy experiments, the colinear configuration

between the NIR pump and the XUV probe pulses has been used [59]. Thus, the

contribution not only from the high (peak) intensity region at the central part of the laser

beam but also the low-intensity region at the wing of the laser beam might be involved in

the XUV spectra. Therefore, we speculate that the contribution of a fast component of Fe^+

formation from the more highly excited states of $FeCp_2^+$ and/or excited $FeCp_2^{2+}$ is masked

by the dominant contribution from the lowest excited state of $FeCp_2^+$.

The appearance of multiply charged metal cations is determined by the ionization

energy (I_E) if the sequential (stepwise) ionization process of a singly charged metal cation

is operative. I_E is the energy required to remove an electron from an atom and/or molecule

with the subsequent production of a positively charged ion. This process can be repeated,

but the ionization energy increases as the charge number increases. The potential energy

I_P that the cation gains is the sum of the ionization energies. I_Es and I_Ps of the transition

metals and xenon are listed in Tables S1 to S6. The I_P values of Cr^{6+}, Fe^{6+}, Ni^{6+}, Ru^{7+},

Os^{8+}, and Xe^{7+} are 263, 283, 299, 325, 403, and 318 eV, respectively. The generation of

those cations from Cr^{5+}, Fe^{5+}, Ni^{5+}, Ru^{6+}, Os^{7+}, and Xe^{6+} requires 90.6, 98.9, 108, 93.0,

102, and 91.6 eV, respectively. Further removal of an electron from Cr^{6+}, Fe^{6+}, Ni^{6+}, Ru^{7+},

Os^{8+}, and Xe^{7+} requires 160, 124, 132, 110, 168, and 105 eV, respectively. Here we refer

to the result of the third-row element, magnesium. Fig. S2 shows the peak of Mg^{3+} in the

mass spectrum of $MgCp_2$, which is the most highly charged magnesium observed at

3.7×10^{15} W cm^{-2}. The I_P of Mg^{3+} (103 eV) is lower than that of the most highly charged

states of the fourth-, fifth-, and sixth-row transition metals (263−403 eV) observed in this

study. The absence of Mg^{4+} (I_P= 212 eV) is probably attributable to the relatively high I_E

of Mg^{3+} (109 eV). In addition, the yield of Mg^{3+}, the precursor of Mg^{4+}, is more than two

orders of magnitude smaller than that of Mg^{2+}, probably due to the high I_E of Mg^{2+} (80.1

eV). Based on the observations of the highest charge states of transition metals, we can

conclude that removing an electron that requires 90.6 (Cr^{5+}) − 108 eV (Ni^{5+}) is possible,

while removing one that requires 110 (Ru^{7+}) − 168 eV (Os^{8+}) does not occur at the peak

laser intensity achieved in this study. It should be noted that these definitions are not

strictly determined because the I_Es of higher charge states have large ambiguities.

Nonetheless, these results indicate that the ionization process is governed not by I_p but by

I_E., i.e., sequential ionization processes of isolated metal cations are operative in intense

femtosecond laser fields. Here we consider about the absence of C^{4+} because the energy

required to remove an electron from C^{3+} is 64.5 eV. C^{4+} should be produced if carbon

atom liberated from ligands is further ionized in the high (peak) intensity region. However, the sequential ionization of carbon atom is not likely because most ligands desorb as neutral fragments in the early stage of ionization. Some ligands might be highly charged and subsequently exploded to form C^{3+}.

3.1. Saturation intensity of metal cations

Fig. 2 shows the metal cation yield as a function of laser intensity. The same plot for $FeCp_2$ was reported previously [53]. We used the saturation intensity (I_{sat}) proposed by Hankin *et al.* [54, 60] to quantitatively compare the production of cations. A typical example of the determination of I_{sat} for the iron cations is shown in Fig. 3. I_{sat} is defined as the point at which the ion yield (linear scale), extrapolated from the high-intensity linear portion of the curve, intersects the intensity axis (logarithmic scale). Good linear lines were obtained for Fe^{z+} ($z = 1-5$), and the intersect gave $I_{sat\ exp}$. We estimated $I_{sat\ exp}$ up to Cr^{5+}, Fe^{5+}, Ni^{5+}, Ru^{6+}, Os^{7+}, and Xe^{6+}, respectively. $I_{sat\ exp}$ of the highest charge state was not obtained due to the insufficient data plots to be extrapolated; for example, Fe^{6+} in Fig. 3. Table 1 lists the $I_{sat\ exp}$ values of transition metals and xenon. Fig. 4a shows the correlation between $I_{sat\ exp}$ and I_E. Although the dependence of the variations on the metals is obvious, it can also be seen that the $I_{sat\ exp}$s are proportional to I_Es. Further, it is clear

14

that the $I_{\text{sat exp}}$s of xenon are higher than those of transition metal cations with the same I_{E}.

The same procedure was used to determine the theoretical values. We assume that the sequential tunnel ionization mechanism is operative for the generation of multiply charged atomic cations. ADK (Ammosov-Delone-Krainov) theory, which is based on the single active electron approximation is known as a simple analytical approach to evaluate ionization rates [61]. ADK theory is applicable to atoms with small sets of parameters; however, ionization theories in intense electric fields have been rapidly developing [62-65], and the limitations and modifications of ADK theory have also been proposed [66, 67]. We understand that more sophisticated theories have been proposed and have successfully described the experimental results for singly charged metal cations [68-70]. However, theoretical calculations of multiply charged metal cations, especially of open-shell atoms, are still challenging even with the recent approaches [71]. In a step toward understanding the production of multiply charged transition metal cations, we will use ADK theory because precise arguments about ionization rates depending on the different theoretical treatments are not within the scope of this study. Since ADK theory can still be used as a benchmark for complex systems [72, 73], it is more important to argue that theoretical values deviate from experimental values rather than to discuss exactly how the theory reproduces experimental values. We will discuss the degree of deviation of $I_{\text{sat ADK}}$,

which is derived from ADK theory, from $I_{\text{sat exp}}$. To evaluate how much the theoretical value deviates from the experimental value, we refer to the results of xenon as a benchmark atom. As the ADK theory can describe the $I_{\text{sat exp}}$ of xenon within a factor of 1.3 [74, 75], a comparison between the results for transition metals and those for xenon would be a rough but good index. The nonsequential ionization (electron rescattering or direct ionization) processes are not considered because the ions produced by those processes are a few orders of magnitude smaller than those produced by the sequential ionization processes [76].

The ADK formula is expressed by an effective principal quantum number n^*, angular momentum quantum number l, and magnetic quantum number m. The ionization rate of an atom in the electric field ε is described by

$$W = C_{n^*l}^2 \, f(l,m) \, \varepsilon_0 \, \sqrt{\frac{3\,\varepsilon}{\pi\,\kappa}} \left(\frac{2\,\kappa}{\varepsilon}\right)^{2n^*-|m|-1} \exp\left(-\frac{2\,\kappa}{3\,\varepsilon}\right) \tag{1}$$

with

$$C_{n^*l} = \frac{1}{\sqrt{2\pi n^*}}\left(\frac{2e}{n^*}\right)^{n^*}, \; f(l,m) = \frac{(2l+1)(l+|m|)!}{2^{|m|}|m|!(l-|m|)!}, \; \kappa = (2\,\varepsilon_0)^{\frac{3}{2}}, \text{ and } n^* = \frac{z}{\sqrt{2\,\varepsilon_0}}.$$

ε_0 and z are the ionization energy and the charge number, respectively. The constant e in coefficient C_{n^*l} is Euler's number. ε_0 and ε are obtained from the experimentally convenient I_E (in eV units) and E (in V m^{-1} units). Consequently, E is derived from laser intensity I (in W cm^{-2} units).

The time evolution and spatial distribution of laser intensity should be considered in the evaluation of ionization rates and hence of ion yields. As an aperture that is shorter than the Rayleigh length is used to restrict ion collection, the integration of ionization rates is constant over the laser propagation direction [77, 78]. The laser intensity profile (Gaussian TEM$_{00}$ mode) in the cylindrical volume is described approximately by

$$I_r = I_0 \exp\left[-\left(\frac{r}{\omega_0}\right)^2\right], \qquad (2)$$

where I_0, r, and ω_0 are the peak laser intensity, the radial distance from the beam axis, and the beam waist radius where $I_r = \frac{I_0}{e}$, respectively. We assume that the time evolution of the laser intensity I_t is described by a Gaussian function

$$I_t = I_0 \exp\left[-4\ln2\left(\frac{t}{\tau}\right)^2\right], \qquad (3)$$

where τ is the pulse duration (fwhm). The ion yield is obtained by

$$S = A \int_0^{I_0} \frac{\left[1-\exp\left\{-\int_{-\infty}^{\infty} W\,dt\right\}\right]}{I_r}\,dI_r, \qquad (4)$$

where A is a constant including the all experimental factors. At the high laser intensity limit, Eq. (4) is expressed by

$$S = A(\ln I_0 - \ln I_{\text{sat}}). \qquad (5)$$

Here we calculated the $I_{\text{sat ADK}}$s of atoms. The values of I_E, z, and l used in the calculations are shown in Tables S1 to S6. We assume that cations are prepared in their

17

ground states and that electron reconfiguration is fast compared to the succeeding

ionization step. We fixed the magnetic quantum number to zero, which gives the lowest

$I_{sat\ ADK}$. The ionization rates, ionization probabilities, and ion yields were calculated using

conventional spreadsheet software (Fig. S3). We fixed τ to 45 fs. Since sufficient

accuracy could be guaranteed, we integrated the range from $-3\ \tau$ to $3\ \tau$.

The calculated ionization probabilities and ion yields as functions of peak laser intensity,

for example, Fe^{z+} ($z = 1-5$), are shown in Fig. 5. $I_{sat\ ADK}$s are summarized in Table 1. Here

we try to compare the $I_{sat\ exp}$ of metals generated from metallocenes with the $I_{sat\ ADK}$ of

metal atoms. To evaluate the deviation of $I_{sat\ ADK}$ from $I_{sat\ exp}$, we plotted the $I_{sat\ ADK}/I_{sat\ exp}$

as a function of the ionization energy of the atoms in Fig. 4b. The results for xenon are

shown as a reference.

$I_{sat\ ADK}/I_{sat\ exp}$s of xenon were slightly larger than or nearly equal to unity, i.e., the

formation of xenon cation required less laser intensity than expected by ADK theory.

These results show that ADK theory overestimates I_{sat} ($I_{sat\ ADK} > I_{sat\ exp}$) and hence

underestimates the ionization rate (ion yield) of xenon as reported in the literature [74,

75]. Yamakawa et al. have reported the shift factors, which are the numbers by which the

theoretical intensity scales have been multiplied to fit the experimental intensity scales

[75]. The reciprocal of $I_{sat\ ADK}/I_{sat\ exp}$s correspond to their shift factors. The average of the

shift factors and the average of the reciprocal of $I_{\text{sat ADK}}/I_{\text{sat exp}}$s for Xe^+ to Xe^{6+} are

0.74±0.12 and 0.82±0.04, respectively. It should be noted that different ionization

energies of xenon were used for the calculations (see Table S6); however, the

phenomenon of ADK theory overestimating the I_{sat} of xenon was confirmed in both cases.

Although the discrepancies between $I_{\text{sat ADK}}$ and $I_{\text{sat exp}}$ for xenon should not be neglected,

those for transition metal cations were more significant. $I_{\text{sat ADK}}/I_{\text{sat exp}}$s of xenon were

nearly independent of the charge numbers. In contrast, those of singly and doubly charged

transition metal cations were less than unity ($I_{\text{sat ADK}} < I_{\text{sat exp}}$), while those of triply and

more highly charged transition metal cations were more than unity ($I_{\text{sat ADK}} > I_{\text{sat exp}}$). In

other words, ADK theory underestimates the former I_{sat}s while overestimating the latter

I_{sat}s.

The origin of singly and presumably doubly charged transition metal cations is the

excited metallocene cation and/or dication. Thus, it is not reasonable to govern the

generation of singly and doubly charged transition metals by the I_{E} of transition metal

atoms. Smits et al. have reported the formation of V^+, Nb^+, Ta^+, Ni^+, and Pd^+ from neutral

metal atoms [79]. They utilized laser ablation to form a neutral metal atomic beam with

helium as the carrier gas followed by ionization with femtosecond laser pulses (90 fs, 1.5

μm). The $I_{\text{sat ADK}}/I_{\text{sat exp}}$s derived from their data were 0.38 (V^+), 0.18 (Nb^+), 0.39 (Ta^+),

0.38 (Ni^+), and 0.42 (Pd^+) [79]. They concluded that the underestimation of I_{sat} by the ADK theory is due to the dynamic polarization or screening effect. In other words, the suppression of ionization is due to the collective movement of electrons toward one side of the potential well, resulting in the repulsion of electrons and consequent increase in the potential barrier. Their results for singly charged metal cations have been well explained by the increase in both the potential barrier and the ionization energy using the generalized ADK theory [68, 70] and time-dependent density functional theory [69]. However, those suggested mechanisms do not explain why the I_{sat} of multiply charged transition metal cations was overestimated by ADK theory.

In contrast to singly and doubly charged transition metal cations, the $I_{sat\ ADK}/I_{sat\ exp}$s of triply and more highly charged transition metals were more than unity. It should be emphasized that the I_{sat} of not only multiply charged iron [53] but also of other multiply charged transition metals are overestimated by the ADK theory. Although the data for Cr^{5+}, Fe^{5+}, Ni^{5+}, and Ru^{5+} were scattered due to the uncertainly of I_{sat}s evaluations, we classified the five transition metals into two groups: fourth- and fifth-row elements (Cr, Fe, Ni, Ru) in one group and a sixth-row element (Os) in the other.

Of course, it should be mentioned that these results show the limits of ADK theory applied to multiply charged transition metal cations. Nonetheless, we have presented the

20

$I_{\text{sat exp}}$s of five transition metals and different trends among different row elements. In the future, these results could be further examined using more sophisticated theories. For now, we can provide some potential insights into the origins of I_{sat} deviations. The static dipole polarizability is an index of an induced dipole moment of an atom in an external electric field [80]. The screening effect in multiply charged metal cations would be reduced since their polarizability dramatically decreases as the charge number increases [81-83]. For example, the polarizabilities of singly and doubly charged cations relative to that of a neutral atom were calculated previously: Cr, 0.11, 5.0×10^{-2}; Fe, 0.44, 7.0×10^{-2}; Ni, 0.12, 5.0×10^{-2}; Ru, 0.14, 7.9×10^{-2} [83]. Although those of Os were not obtained, those of sixth-row elements showed trends similar to those of Xe: Xe, 0.63, 0.43; Eu, 0.48, 0.18; Yb, 0.52, 0.22; Hf, 0.45, 0.28 [83]. We expect that the degree to which polarizability is reduced will become much more significant between transition metals and Xe in higher charge states [81]. This trend should also be important for the long-range interaction between tunneling and bound electrons as well as for the laser-induced Stark shift, both of which are proposed as the origins of the overestimation of ionization rate (underestimation of I_{sat}) by the ADK theory for singly charged transition metals [68, 70]. It is certain that the polarizabilities are key factors determining tunnel ionization behavior; however, further theoretical consideration is beyond the scope of this study.

We could discuss the degree of the underestimation based on the tunneling barrier and effective ionization energy. However, the literature makes no attempt to explain the overestimation of I_{sat} of isolated atoms. We should mention that the overestimation of I_{sat} referred to as an "enhanced ionization" has been reported for various metal clusters [55-58, 84-89] as well as for nonmetal clusters [90, 91]. The origin of enhancement is intracluster interactions resulting in large kinetic energy releases. However, the interactions between metals [57] leading to enhanced ionization are not expected for isolated metallocenes. A possible and simple explanation for the overestimation of I_{sat} could be the reduction of ionization energy by the excitation of cations. Fig. S5 shows the atomic spectra of Cr^+, Fe^+, and Ni^+ taken from the literature. Those of Ru^+ and Os^+ were not available. There are innumerable atomic absorption lines at around 800 nm in the cases of Fe^+ and Ni^+. It is expected that the photoexcitation of cations reduces the energy for ionization, which in turn may enhance the ionization rate. In contrast, the atomic lines of Xe^+, Xe^{2+}, and Xe^{3+} at around 800 nm are rather sparse (Fig. S6). Since the I_Es of singly charged cations are less than 10 eV, the photoexcitation (1.55 eV/photon) would significantly alter the ionization rates. However, the reduction of I_E by only a few eVs might not significantly influence the production of multiply charged cations that occurs in a tunneling intensity regime. For example, the reductions in I_Es by 21 eV and 16 eV

22

are necessary in order to make the $I_{\text{sat ADK}}$s equal to the $I_{\text{sat exp}}$s of Ru^{5+} and Os^{6+}, respectively. Alternatively, the collision between an ion core and an electron, which is accelerated by laser electric fields, may be attributable to the excitation [92]. Since the ponderomotive energy at 10^{15} W cm^{-2} is 60 eV, the maximum collisional energy is expected to be 190 eV. Cations could gain significantly higher energy by the collision with an accelerated elecron; however, the efficiency of such an excitation would likely be too low, since the deviations in ADK expectations from the experimental results are independent of the charge number in the case of Xe. Further experiments for various metals using different wavelengths and/or circularly polarized laser pulses will lead to the accumulation of valuable information for theoretical arguments.

4. Conclusion

By using the corresponding metallocenes as reactants, we have shown that femtosecond laser ionization produces multiply charged metal cations by a low ambient temperature process. The potential use of different reactants is another benefit of this method. We can expand the range of metals by using other metallocenes. For example, we produced Hf^{7+} from hafnocene dichloride at 2×10^{15} W cm^{-2} (Fig. S4). Since the metallocene is

sandwich-shaped whereas metallocene dichloride has a bent shape, a simple comparison could not be performed.

We have found that osmium shows a different ionization trend among the group VIII transition metals (Fe, Ru, Os). The origin of this difference is not certain, but we suggest it might be important that the trends in polarizability upon multiple ionizations of sixth-row elements (transition metals and lanthanides) differ from those of other transition metals but are similar to those of Xe. In multiply charged states, the nature of the orbitals of the remaining electrons should be important for clarifying the multiple-tunneling ionization processes. Further studies, focusing on the differences in multiple ionization behaviors of the same group but with different row elements, are necessary to gain further insight into the multiple ionization processes of transition metals in intense laser fields. We can use metallocene dichlorides to examine group IV metals (Ti, Zr, Hf). Since the amounts of carbon and of chloride cations are small, it is expected that multiply charged metal cations are formed by the ionization of liberated metals from the excited states of metallocene dichlorides as in the cases of metallocenes. Although the main focus is the Coulomb explosion of ligands, we previously reported the production of Cr^{5+}, Mo^{5+}, and W^{6+} from the corresponding fourth-, fifth-, and sixth-row carbonyl complexes of group VI metals in intense femtosecond laser fields [93]. The production of singly charged

group V metals of fourth- and sixth-row elements (V, Ta) has been well described by the generalized ADK theory, while that of the fifth-row element (Nb) is far from the expectation by generalized ADK theory [68, 70]. The multiple ionization of group V metals might be a key to clarifying the ionization behaviors of transition metals. A systematic study of the ionization of the metals using other series of metallocenes as well as alkyl and carbonyl complexes is in progress.

Appendix A. Supplementary data

Supplementary data associated with this article can be found, in the online version, at XXXX.

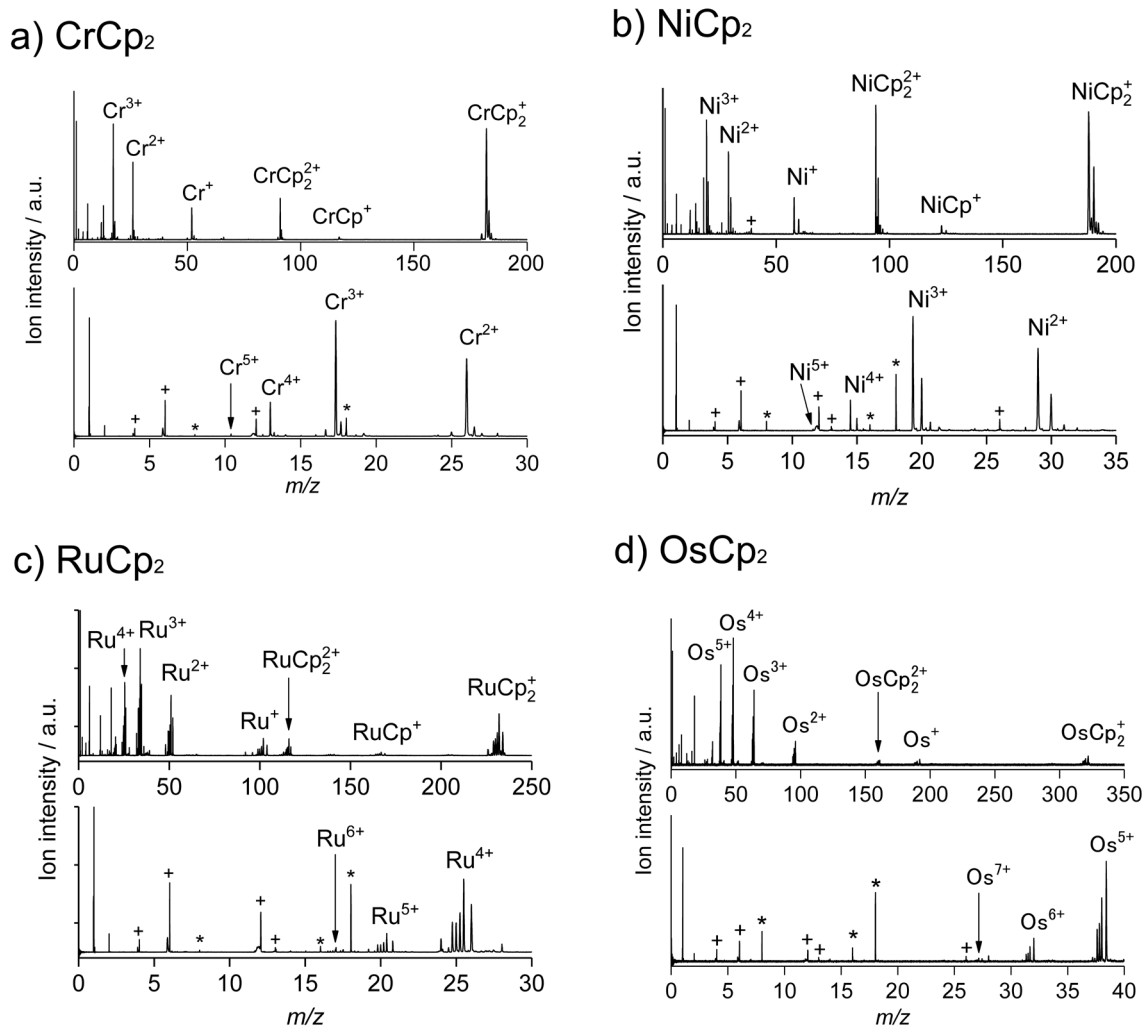**Fig. 1.** Time-of-flight mass spectra of (a) CrCp₂, (b) NiCp₂, (c) RuCp₂, and (d) OsCp₂. Laser intensities are (a) 4.6×10^{15}, (b) 3.9×10^{15}, (c) 3.0×10^{15}, and (d) 4.2×10^{15} Wcm^{-2}, respectively. The laser polarization is parallel to the ion flight axis. The asterisks indicate the ions originating from contaminated water. The pluses indicate the carbon ions originating from cyclopentadienyl ligands.
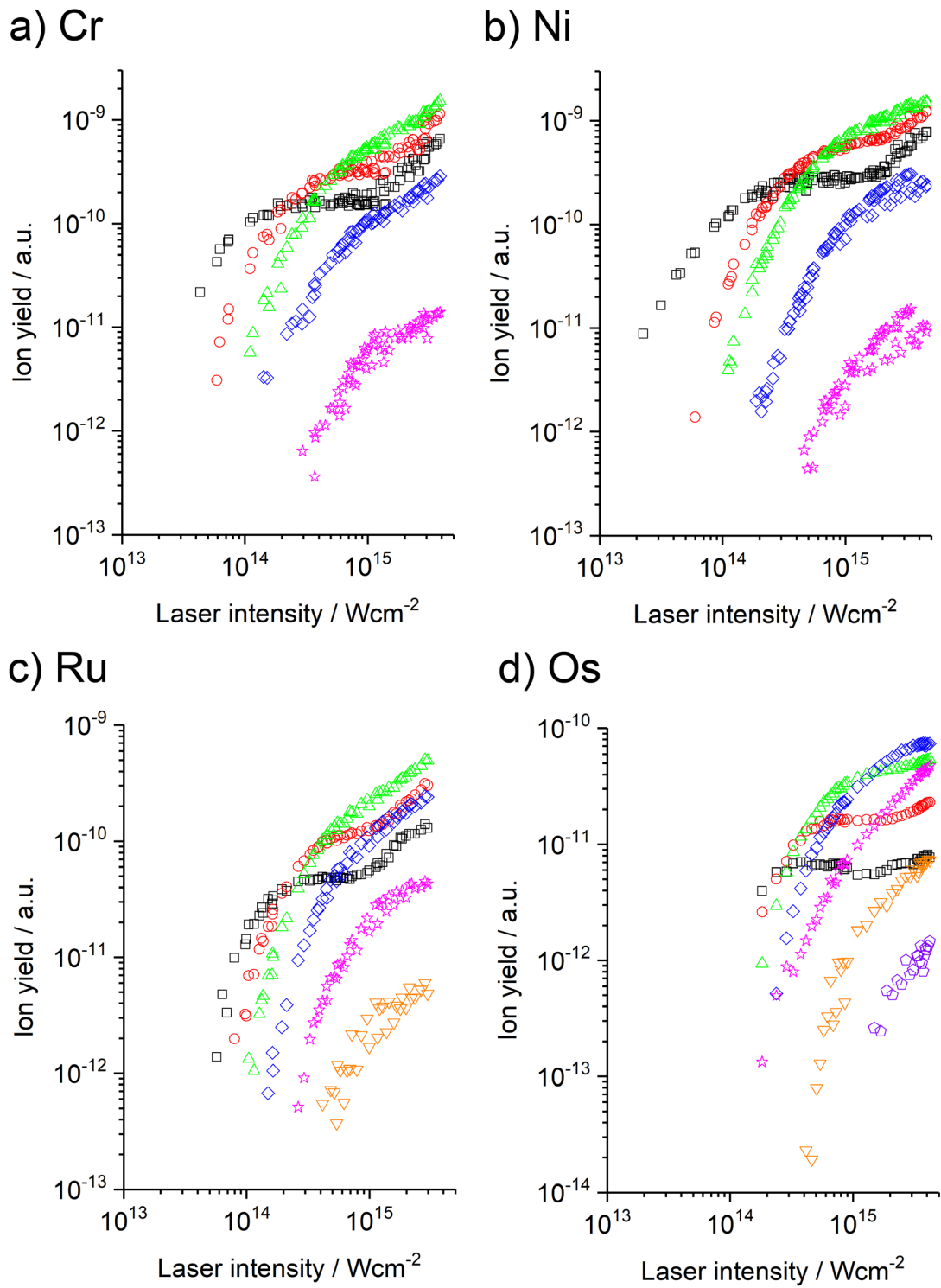
Fig. 2. Metal ion yields as a function of laser intensity: a) Cr^{Z+}, b) Ni^{Z+}, c) Ru^{Z+}, and d) Os^{Z+}. $z = 1$ (squares), 2 (circles), 3 (triangles), 4 (diamonds), 5 (stars), 6 (inverted triangles), and 7 (pentagons).
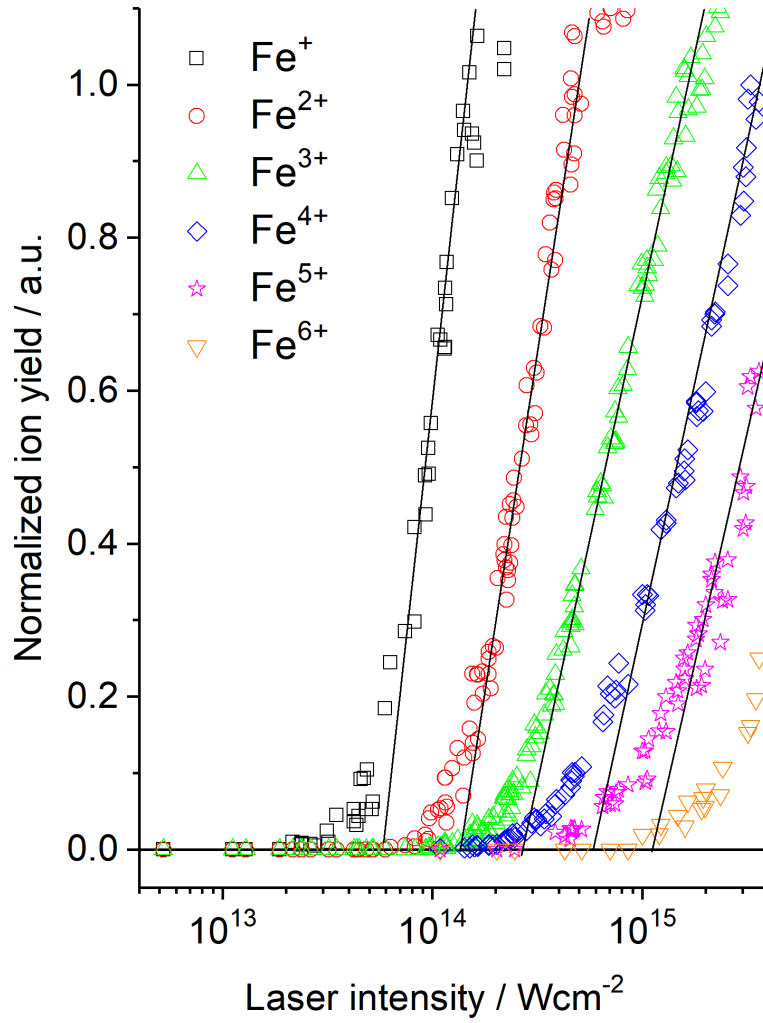
Fig. 3. Correlation between the yield of Fe^{z+} and the logarithm of the laser intensity. The solid linear lines are the extrapolation from the high-intensity linear portions of the plots. The intersection with the intensity axis gives $I_{\text{sat exp.}}$ $z = 1$ (squares), 2 (circles), 3 (triangles), 4 (diamonds), 5 (stars), and 6 (inverted triangles).
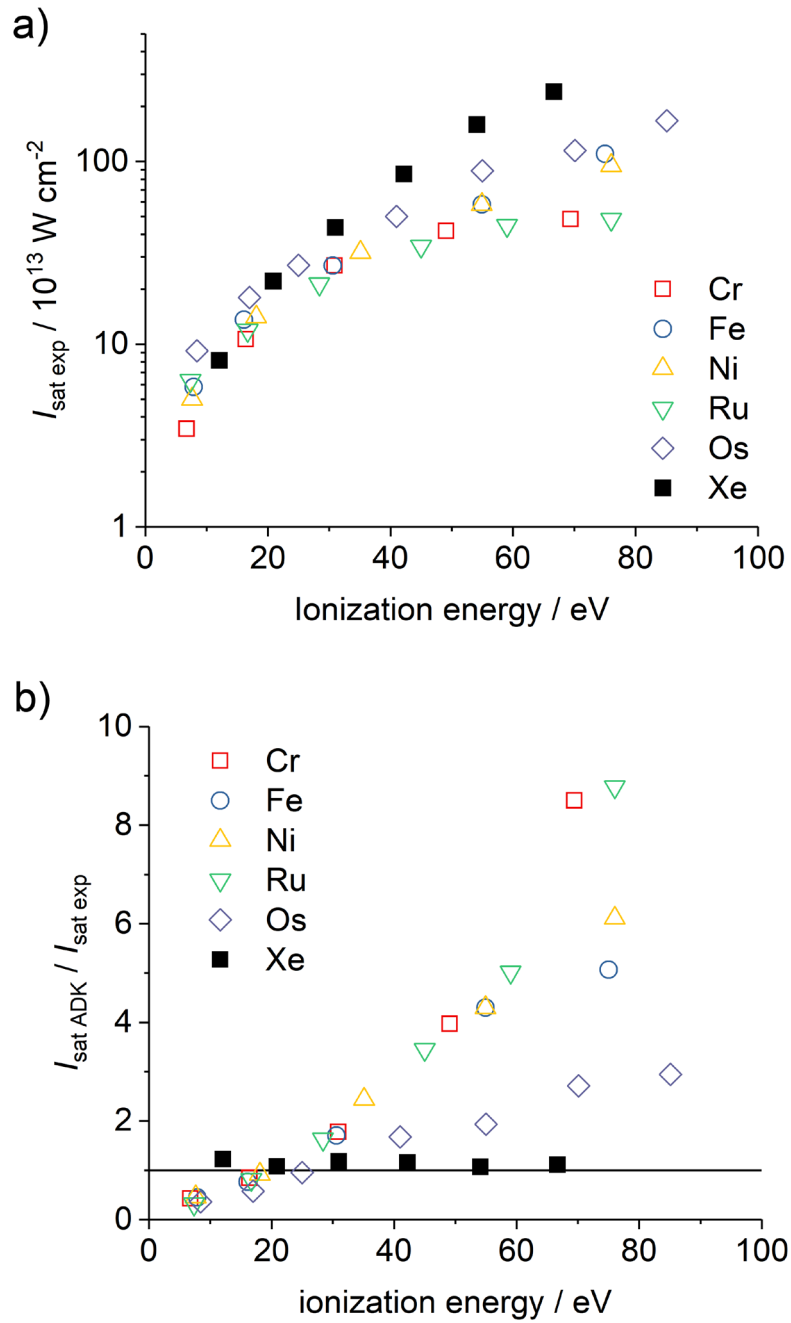
Fig. 4. (a) $I_{sat\ exp}$ as a function of the ionization energy of elements. (b) The ratio of theoretically estimated $I_{sat\ ADK}$ to experimentally obtained $I_{sat\ exp}$ as a function of the ionization energy of elements: Cr (squares); Fe (circles); Ni (triangles); Ru (inverted triangles); Os (diamonds); Xe (filled squares).
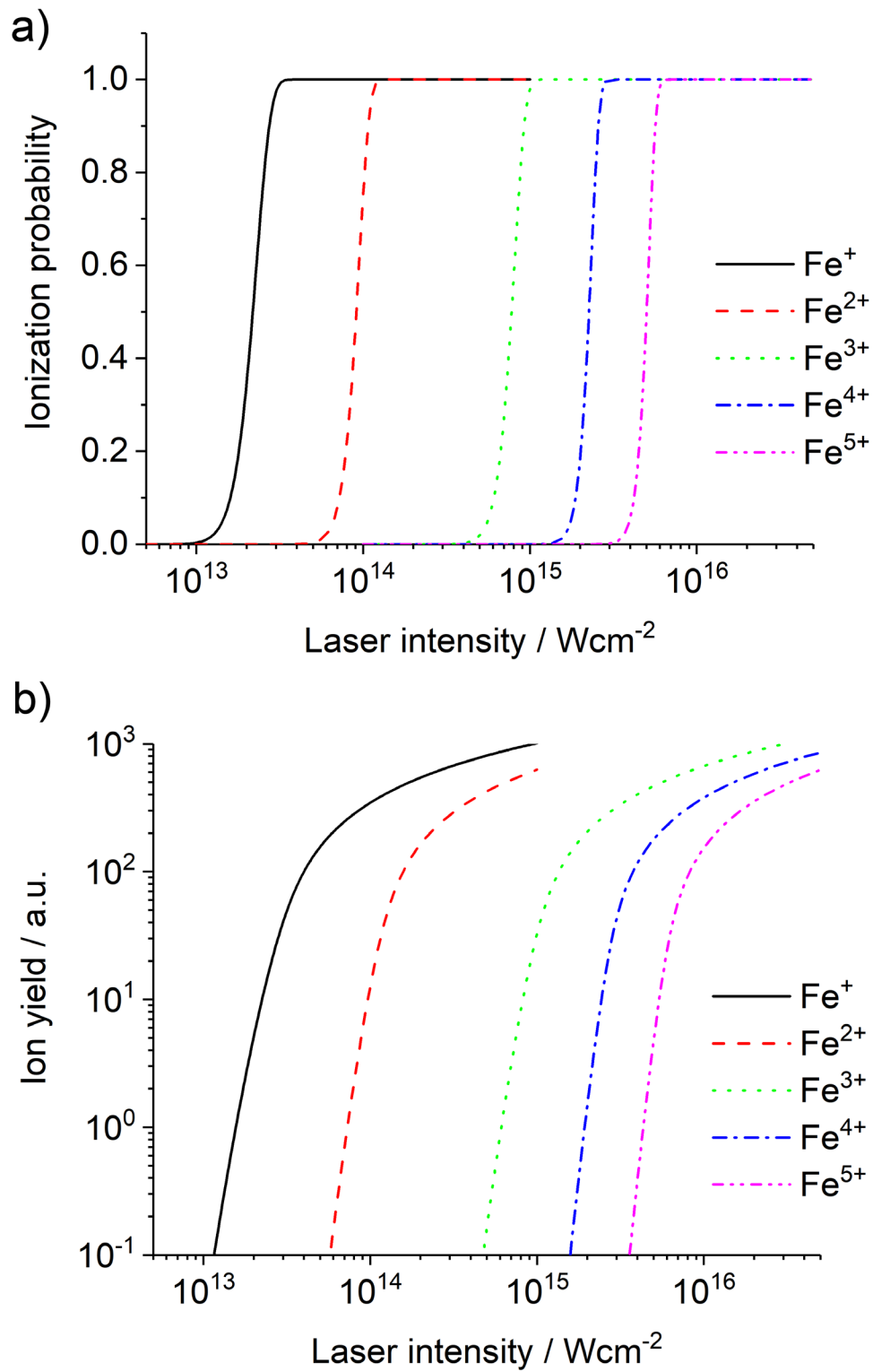
Fig. 5. Calculated (a) ionization probabilities and (b) ion yields of Fe^{z+} ($z = 1-5$).

Table 1

Saturation intensity (I_{sat}/ 10^{13} W cm^{-2}) of metal cations M^{z+}.[a]

z	1	2	3	4	5	6	7
Cr^{z+}	3.4	11	27	42	48		
	1.5	9.0	48	165	411		
Fe^{z+}	5.8	14	27	58	110		
	2.6	10	46	250	557		
Ni^{z+}	5.0	14	32	58	95		
	2.3	13	78	250	581		
Ru^{z+}	6.3	12	21	34	45	48	
	2.0	9.7	35	119	224	423	
Os^{z+}	9.2	18	27	50	89	115	167
	3.3	10	26	84	172	312	492
Xe^{z+}	8.1	22	44	86	159	241	
	10	24	51	99	170	268	

[a] $I_{sat\ exp}$ and $I_{sat\ ADK}$ are shown in upper and lower column, respectively.

References

[1] P.B. Armentrout, Electronic state-specific transition-metal ion chemistry, Annu. Rev. Phys. Chem., 41 (1990) 313-344.

[2] P.B. Armentrout, Reactions and thermochemistry of small transition metal cluster ions, Annu. Rev. Phys. Chem., 52 (2001) 423-461.

[3] J. Roithová, D. Schröder, Selective activation of alkanes by gas-phase metal ions, Chem. Rev., 110 (2010) 1170-1211.

[4] D.K. Bohme, H. Schwarz, Gas-phase catalysis by atomic and cluster metal ions: The ultimate single-site catalysts, Angew. Chem. Int. Ed., 44 (2005) 2336-2354.

[5] E. Herbst, Chemistry in the interstellar-medium, Annu. Rev. Phys. Chem., 46 (1995) 27-53.

[6] D.K. Bohme, PAH and fullerene ions and ion molecule reactions in interstellar and circumstellar chemistry, Chem. Rev., 92 (1992) 1487-1508.

[7] S. Petrie, D.K. Bohme, Ions in space, Mass Spectrom. Rev., 26 (2007) 258-280.

[8] M. Larsson, W.D. Geppert, G. Nyman, Ion chemistry in space, Rep. Prog. Phys., 75 (2012) 066901.

[9] R. Zenobi, R. Knochenmuss, Ion formation in MALDI mass spectrometry, Mass Spectrom. Rev., 17 (1998) 337-366.

[10] P.B. Armentrout, Kinetic energy dependence of ion-molecule reactions: Guided ion beams and threshold measurements, Int. J. Mass Spectrom., 200 (2000) 219-241.

[11] P.B. Armentrout, Fifty years of ion and neutral thermochemistry by mass spectrometry, Int. J. Mass Spectrom., 377 (2015) 54-63.

[12] N.M.M. Nibbering, Gas-phase ion molecule reactions as studied by Fourier-transform ion-cyclotron resonance, Acc. Chem. Res., 23 (1990) 279-285.

[13] S. Kazazic, L. Klasinc, S.P. McGlynn, D. Srzic, M.G.H. Vicente, Gas-phase metallation reactions of porphyrins with metal monocations, J. Phys. Chem. A, 108 (2004) 10997-11000.

[14] L.G. Parke, C.S. Hinton, P.B. Armentrout, Energetics and mechanisms of C-H bond activation by a doubly charged metal ion: Guided ion beam and theoretical studies of Ta^{2+} + CH_4, J. Phys. Chem. A, 112 (2008) 10469-10480.

[15] J.D. Fletcher, M.A. Parkes, S.D. Price, Bond-forming reactions of small triply charged Cations with neutral molecules, Chem. Eur. J., 19 (2013) 10965-10970.

[16] S.D. Price, Coincidence studies of the bond-forming reactivity and reaction dynamics of molecular dications, Int. J. Mass Spectrom., 260 (2007) 1-19.

[17] M.A. Parkes, J.F. Lockyear, S.D. Price, Reactions of O_2^{2+} with CO_2, OCS and CS_2,

Int. J. Mass Spectrom., 354 (2013) 39-45.

[18] J. Roithová, D. Schröder, Bond-forming reactions of molecular dications as a new route to polyaromatic hydrocarbons, J. Am. Chem. Soc., 128 (2006) 4208-4209.

[19] J. Jasik, J. Roithová, J. Zabka, R. Thissen, I. Ipolyi, Z. Herman, Dynamics of chemical and charge transfer reactions of molecular dications: VI reactions of $C_4H_3^{2+}$ with Kr, Xe, H-2, N-2, NO, NH3, C2H2, and CH4, Int. J. Mass Spectrom., 255 (2006) 150-163.

[20] D. Mathur, Multiply charged molecules, Phys. Rep., 225 (1993) 193-272.

[21] D. Mathur, Structure and dynamics of molecules in high charge states, Phys. Rep., 391 (2004) 1-118.

[22] K. Vekey, Multiply charged ions, Mass Spectrom. Rev., 14 (1995) 195-225.

[23] D. Schroder, H. Schwarz, Generation, stability, and reactivity of small, multiply charged ions in the gas phase, J. Phys. Chem. A, 103 (1999) 7385-7394.

[24] M.M. Bursey, P.F. Rogerson, J.M. Bursey, Quadruply charged ions in mass spectrum of ovalene, Org. Mass Spectrom., 4 (1970) 615-617.

[25] R.G. Kingston, M. Guilhaus, A.G. Brenton, J.H. Beynon, Multiple ionization, charge separation and charge stripping reactions involving polycyclic aromatic compounds, Org. Mass Spectrom., 20 (1985) 406-412.

[26] D.A. Hagan, J.H.D. Eland, Formation and decay of doubly charged ions from polycyclic aromatic-hydrocarbons and related-compounds, Rapid Commun. Mass Spectrom., 5 (1991) 512-517.

[27] A. Lawicki, A.I.S. Holm, P. Rousseau, M. Capron, R. Maisonny, S. Maclot, F. Seitz, H.A.B. Johansson, S. Rosen, H.T. Schmidt, H. Zettergren, B. Manil, L. Adoui, H. Cederquist, B.A. Huber, Multiple ionization and fragmentation of isolated pyrene and coronene molecules in collision with ions, Phys. Rev. A, 83 (2011) 022704.

[28] P. Rousseau, A. Lawicki, A.I.S. Holm, M. Capron, R. Maisonny, S. Maclot, E. Lattouf, H.A.B. Johansson, F. Seitz, A. Mery, J. Rangama, H. Zettergren, S. Rosen, H.T. Schmidt, J.Y. Chesnel, A. Domaracka, B. Manil, L. Adoui, H. Cederquist, B.A. Huber, Low-energy ions interacting with anthracene molecules and clusters, Nucl. Instrum. Meth. B, 279 (2012) 140-143.

[29] V. Brites, K. Franzreb, J.N. Harvey, S.G. Sayres, M.W. Ross, D.E. Blumling, A.W. Castleman, M. Hochlaf, Oxygen-containing gas-phase diatomic trications and tetracations: ReO^{z+}, NbO^{z+} and HfO^{z+} (z=3, 4), Phys. Chem. Chem. Phys., 13 (2011) 15233-15243.

[30] K. Franzreb, J. Hrusak, M.E. Alikhani, J. Lorincik, R.C. Sobers, P. Williams, Gas-phase diatomic trications of Se_2^{3+}, Te_2^{3+}, and LaF^{3+}, J. Chem. Phys., 121 (2004) 12293-

12302.

[31] K.W.D. Ledingham, R.P. Singhal, D.J. Smith, T. McCanny, P. Graham, H.S. Kilic, W.X. Peng, S.L. Wang, A.J. Langley, P.F. Taday, C. Kosmidis, Behavior of polyatomic molecules in intense infrared laser beams, J. Phys. Chem. A, 102 (1998) 3002-3005.

[32] T. Yatsuhashi, N. Nakashima, Formation and fragmentation of quadruply charged molecular ions by intense femtosecond laser pulses, J. Phys. Chem. A, 114 (2010) 7445-7452.

[33] T. Yatsuhashi, N. Mitsubayashi, M. Itsukashi, M. Kozaki, K. Okada, N. Nakashima, Persistence of iodines and deformation of molecular structure in highly charged diiodoacetylene: anisotropic carbon ion emission, ChemPhysChem, 12 (2011) 122-126.

[34] T. Yatsuhashi, K. Toyota, N. Mitsubayashi, M. Kozaki, K. Okada, N. Nakashima, Intact four-atom organic tetracation stabilized by charge localization in the gas phase, ChemPhysChem, 17 (2016) 2977-2981.

[35] M. Murakami, R. Mizoguchi, Y. Shimada, T. Yatsuhashi, N. Nakashima, Ionization and fragmentation of anthracene with an intense femtosecond laser pulse at 1.4 μm, Chem. Phys. Lett., 403 (2005) 238-241.

[36] T. Yatsuhashi, N. Nakashima, Effects of polarization of 1.4 μm femtosecond laser pulses on the formation and fragmentation of naphthalene molecular ions compared at the same effective ionization intensity, J. Phys. Chem. A, 109 (2005) 9414-9418.

[37] N. Mitsubayashi, T. Yatsuhashi, H. Tanaka, S. Furukawa, M. Kozaki, K. Okada, N. Nakashima, Anisotropic Coulomb explosion of acetylene and diacetylene derivatives, Int. J. Mass Spectrom., 403 (2016) 43-52.

[38] V.R. Bhardwaj, P.B. Corkum, D.M. Rayner, Internal laser-induced dipole force at work in C_{60} molecule, Phys. Rev. Lett., 91 (2003) 203004.

[39] N. Nakashima, S. Shimizu, T. Yatsuhashi, S. Sakabe, Y. Izawa, Large molecules in high-intensity laser fields, J. Photochem. Photobiol. C, 1 (2000) 131-143.

[40] T. Yatsuhashi, N. Nakashima, Multiple ionization and Coulomb explosion of molecules, molecular complexes, clusters and solid surfaces, J. Photochem. Photobiol. C, 34 (2018) 52-84.

[41] T. Yatsuhashi, N. Nakashima, Dissociation and multiply charged silicon ejection in high abundance from hexamethyldisilane, J. Phys. Chem. A, 114 (2010) 11890-11895.

[42] P. Ecija, M.N.S. Rayo, R. Martinez, B. Sierra, C. Redondo, F.J. Basterretxea, F. Castano, Fundamental processes in nanosecond pulsed laser ablation of metals in vacuum, Phys. Rev. A, 77 (2008) 032904.

[43] H. Koivisto, J. Arje, M. Nurmia, Metal-Ion Beams from an Ecr Ion-Source Using Volatile Compounds, Nucl. Instrum. Meth. B, 94 (1994) 291-296.

[44] J. Opitz, D. Bruch, G. Vonbunau, Multiphoton excitation of ferrocene and vanadocene at 351 nm in comparison with 248 nm and 193 nm. Wavelength dependent competition between ionization and dissociation, Org. Mass Spectrom., 28 (1993) 405-411.

[45] J. Opitz, P. Harter, Multiphoton ionization of vanadocene and ferrocene at 248 nm and 193 nm. Wavelength-dependent competition between dissociation and ionization, Int. J. Mass Spectrom., 121 (1992) 183-199.

[46] S. Leutwyler, U. Even, J. Jortner, Multiphoton dissociation and ionization of metallocenes cooled in supersonic beams, J. Phys. Chem., 85 (1981) 3026-3029.

[47] S.Y. Ketkov, H.L. Selzle, E.W. Schlag, S.N. Titova, Multiphoton ionization of jet-cooled nickelocene with tunable nanosecond laser pulses, Chem. Phys., 293 (2003) 91-97.

[48] J.E. Braun, H.J. Neusser, P. Harter, M. Stockl, Dissociative intramolecular charge transfer after local two-photon ionization of ferrocene derivatives with aromatic chromophores, J. Phys. Chem. A, 104 (2000) 2013-2019.

[49] F.J. Currell, The physics of multiply and highly charged ions: interactions with matter, Kluwer Academic Publishers, Dordrecht ; Boston, 2003.

[50] F.J. Currell, The physics of multiply and highly charged ions: sources, applications and fundamental processes, Kluwer Academic Publishers, Dordrecht ; Boston, 2003.

[51] S.L. Bogomolov, A.E. Bondarchenko, A.A. Efremov, K.I. Kuzmenkov, A.N. Lebedev, K.V. Lebedev, V.Y. Lebedev, V.N. Loginov, V.E. Mironov, N.Y. Yazvitsky, Production of intense metal ion beams from ECR ion sources using the MIVOC method, Phys. Part. Nuclei Lett., 12 (2015) 824-830.

[52] T. Nakagawa, J. Arje, Y. Miyazawa, M. Hemmi, T. Chiba, N. Inabe, M. Kase, T. Kageyama, O. Kamigaito, A. Goto, M.G. Niimura, Y. Yano, Production of highly charged metal ion beams from organic metal compounds at RIKEN 18GHz ECRIS, Nucl Instrum Meth A, 396 (1997) 9-12.

[53] T. Yatsuhashi, E. Murakami, N. Nakashima, Fe^{z+} (z=1-6) generation from ferrocene, Phys. Chem. Chem. Phys., 13 (2011) 4234-4238.

[54] S.M. Hankin, D.M. Villeneuve, P.B. Corkum, D.M. Rayner, Intense-field laser ionization rates in atoms and molecules, Phys. Rev. A, 64 (2001) 013405.

[55] D.E. Blumling, S.G. Sayres, A.W. Castleman, Strong-field ionization and dissociation studies of small early transition metal oxide clusters, Int. J. Mass Spectrom., 300 (2011) 74-80.

[56] D.E. Blumling, S.G. Sayres, A.W. Castleman, Strong-field ionization and dissociation studies on small early transition metal carbide clusters via time-of-flight

mass spectrometry, J. Phys. Chem. A, 115 (2011) 5038-5043.

[57] D.E. Blumling, S.G. Sayres, M.W. Ross, A.W. Castleman, Strong-field ionization of small niobium and tantalum clusters, Int. J. Mass Spectrom., 333 (2013) 55-58.

[58] M.W. Ross, A.W. Castleman, Extreme ionization leading to Coulomb explosion of small palladium and zirconium oxide clusters and reactivity with carbon monoxide, J. Phys. Chem. A, 117 (2013) 1030-1034.

[59] A.S. Chatterley, F. Lackner, C.D. Pemmaraju, D.M. Neumark, S.R. Leone, O. Gessner, Dissociation dynamics and electronic structures of highly excited ferrocenium ions studied by femtosecond XUV absorption spectroscopy, J. Phys. Chem. A, 120 (2016) 9509-9518.

[60] S.M. Hankin, D.M. Villeneuve, P.B. Corkum, D.M. Rayner, Nonlinear ionization of organic molecules in high intensity laser fields, Phys. Rev. Lett., 84 (2000) 5082-5085.

[61] M.V. Ammosov, N.B. Delone, V.P. Krainov, Tunnel ionization of complex atoms and of atomic ions in an alternating electromagnetic field, Sov. Phys. JETP, 64 (1986) 1191-1194.

[62] Y.H. Lai, J.L. Xu, U.B. Szafruga, B.K. Talbert, X.W. Gong, K.K. Zhang, H. Fuest, M.F. Kling, C.I. Blaga, P. Agostini, L.F. DiMauro, Experimental investigation of strong-field-ionization theories for laser fields from visible to midinfrared frequencies, Phys. Rev. A, 96 (2017) 063417.

[63] D. Hochstuhl, C.M. Hinz, M. Bonitz, Time-dependent multiconfiguration methods for the numerical simulation of photoionization processes of many-electron atoms, Eur Phys J-Spec Top, 223 (2014) 177-336.

[64] B.M. Karnakov, V.D. Mur, S.V. Popruzhenko, V.S. Popov, Current progress in developing the nonlinear ionization theory of atoms and ions, Phys. Usp., 58 (2015) 3-32.

[65] S.V. Popruzhenko, Keldysh theory of strong field ionization: history, applications, difficulties and perspectives, J. Phys. B, 47 (2014) 204001.

[66] X.M. Tong, Z.X. Zhao, C.D. Lin, Theory of molecular tunneling ionization, Phys. Rev. A, 66 (2002) 033402.

[67] T. Brabec, M. Cote, P. Boulanger, L. Ramunno, Theory of tunnel ionization in complex systems, Phys. Rev. Lett., 95 (2005) 073001.

[68] Z.X. Zhao, T. Brabec, Tunnel ionization of open-shell atoms, J. Phys. B, 39 (2006) L345-L351.

[69] X. Chu, G.C. Groenenboom, Time-dependent density-functional-theory study of the suppressed tunneling ionization of vanadium, Phys. Rev. A, 94 (2016) 053417.

[70] Z.X. Zhao, T. Brabec, Tunnel ionization in complex systems, J. Mod. Optic, 54 (2007) 981-997.

[71] K. Jivesh, S. Olga, Looking inside the tunnelling barrier: I. Strong field ionisation from orbitals with high angular momentum in circularly polarised fields, J. Phys. B, 51 (2018) 174001.

[72] M. Tanaka, M. Murakami, T. Yatsuhashi, N. Nakashima, Atomiclike ionization and fragmentation of a series of CH_3-X (X : H, F, Cl, Br, I, and CN) by an intense femtosecond laser, J. Chem. Phys., 127 (2007).

[73] T. Yatsuhashi, T. Obayashi, M. Tanaka, M. Murakami, N. Nakashima, Femtosecond laser ionization of organic amines with very low ionization potentials: Relatively small suppressed ionization features, J. Phys. Chem. A, 110 (2006) 7763-7771.

[74] K. Yamakawa, Y. Akahane, Y. Fukuda, M. Aoyama, N. Inoue, H. Ueda, Ionization of many-electron atoms by ultrafast laser pulses with peak intensities greater than 10^{19} W/cm^2, Phys. Rev. A, 68 (2003) 065403.

[75] K. Yamakawa, Y. Akahane, Y. Fukuda, M. Aoyama, N. Inoue, H. Ueda, T. Utsumi, Many-electron dynamics of a Xe atom in strong and superstrong laser fields, Phys. Rev. Lett., 92 (2004) 123001.

[76] S. Larochelle, A. Talebpour, S.L. Chin, Non-sequential multiple ionization of rare gas atoms in a Ti : Sapphire laser field, J. Phys. B, 31 (1998) 1201-1214.

[77] J.H. Posthumus, The dynamics of small molecules in intense laser fields, Rep. Prog. Phys., 67 (2004) 623-665.

[78] J. Posthumus, Molecules and clusters in intense laser fields, Cambridge University Press, Cambridge; New York, 2001.

[79] M. Smits, C.A. de Lange, A. Stolow, D.M. Rayner, Absolute ionization rates of multielectron transition metal atoms in strong infrared laser fields, Phys. Rev. Lett., 93 (2004) 213003.

[80] J. Mitroy, M.S. Safronova, C.W. Clark, Theory and applications of atomic and ionic polarizabilities, J. Phys. B, 43 (2010) 202001.

[81] V.P. Shevelko, A.V. Vinogradov, Static dipole polarizability of atoms and ions in the Thomas-Fermi model, Phys. Scr., 19 (1979) 275-282.

[82] V.P. Shevelko, A.D. Ulantsev, Static multipole polarizability of atoms and ions in the Thomas-Fermi model, J Russ Laser Res, 15 (1994) 529-545.

[83] S.H. Patil, Thomas-fermi model electron density with correct boundary conditions: Applications to atoms and ions, At. Data Nucl. Data Tables, 71 (1999) 41-68.

[84] S.G. Sayres, M.W. Ross, A.W. Castleman, Delocalized electronic behavior observed in transition metal oxide clusters under strong-field excitation, J. Chem. Phys., 135 (2011) 054312.

[85] M.W. Ross, A.W. Castleman, Ultrafast ionization and subsequent coulomb explosion

of zirconium oxide and tungsten carbide "superatomic" cluster species and comparison to group 10 metals, New J. Chem., 36 (2012) 2253-2259.

[86] M.W. Ross, A.W. Castleman, Ionization and Coulomb explosion of small group 10 transition metal oxide clusters in strong light fields, J. Chem. Phys., 137 (2012) 084307.

[87] M.W. Ross, A.W. Castleman, Femtosecond ionization and Coulomb explosion of small transition metal carbide clusters, Chem. Phys. Lett., 547 (2012) 13-20.

[88] M.W. Ross, A.W. Castleman, Ionization and Coulomb explosion of small uranium oxide clusters, J. Phys. B, 45 (2012) 205102.

[89] M.W. Ross, A.W. Castleman, Strong-field ionization and Coulomb explosion of small neodymium and europium oxide clusters, Chem. Phys. Lett., 565 (2013) 22-27.

[90] S.G. Sayres, M.W. Ross, A.W. Castleman, Onset of Coulomb explosion in small silicon clusters exposed to strong-field laser pulses, New. J. Phys., 14 (2012) 055014.

[91] M.W. Ross, C. Berkdemir, A.W. Castleman, Strong-Field Ionization and Coulomb Explosion of Chlorine Weakly Bound to Small Water Clusters, J. Phys. Chem. A, 116 (2012) 8530-8538.

[92] P.B. Corkum, Plasma Perspective on Strong-Field Multiphoton Ionization, Phys. Rev. Lett., 71 (1993) 1994-1997.

[93] H. Tanaka, N. Nakashima, T. Yatsuhashi, Anisotropic Coulomb explosion of CO ligands in group 6 metal hexacarbonyls: $Cr(CO)_6$, $Mo(CO)_6$, $W(CO)_6$, J. Phys. Chem. A, 120 (2016) 6917-6928.